International Research Journal of Advanced Engineering and Science
ISSN (Online): 2455-9024

On Absorbing Coefficient and Acoustic Damping Ratio of Closed Small Space

Kunihiko Ishihara[1], Yuka Yamashita[1], Yuki Oe[2]
[1]Dept. of Clinical Engineering, Tokushima Bunri University, Takamatsu, Kagawa, Japan-769-2193
[2]Dept. of Life Science, Tokushima Pref. Industrial Tech. Center, Tokushima, Tokushima, Japan-770-8021

Abstract**—***Issues related to the sound environment in the medical field are becoming more prominent with advancements in medical care. Noise during sleep and recuperation affects sleep quality, while noise during waking hours and work can cause various physiological disorders and impair cognitive function. Improving the sound environment to facilitate better focus on treatment and creating spaces where medical information can be accurately communicated and understood are necessary areas of research from diverse perspectives. Recently, noise in Neonatal Intensive Care Units (NICUs) has been identified as a significant source of stress for newborns, and noise reduction has become a critical requirement. However, while there have been investigations from a medical perspective, attempts to reduce noise from an engineering standpoint are lacking. The problem of noise entering the incubator from outside, along with the acoustic characteristics within the incubator space such as resonant frequency and sound pressure level (SPL) are not well understood. Moreover, methods for reducing noise in these settings have not been adequately studied. Various measurement methods, such as those using an acoustic tube and a reverberation room, yield different results, leading to uncertainty about which sound absorption coefficient data should be used to reduce SPL inside an incubator with absorbing materials. The purpose of this study is to determine the resonant frequency of the incubator space, the acoustic damping ratio that controls the SPL inside the incubator, and the absorption coefficient needed to reduce the SPL. The absorption coefficient is calculated using the Eyring formula and the reverberation time measured in a space with varying amounts of absorbing material. As a result, we found that the absorption coefficient in sound absorbing micro space is independent of frequency, but that of absorbent itself is depand on the frequency like conventional results.*

Keywords**—** *Acoustic damping ratio,Resonant frequency,Sound Absorption Coefficient, Sound Pressure Level, Sealed Small Space.*

I. Introduction

The issue of acoustic environments in medical settings has become more serious with the advancement of medical care. Noise during sleep or recovery can affect the quality of sleep, and noise during wakefulness or work can lead to various physiological disorders and reduced performance. Improving the acoustic environment to allow patients to focus on treatment, and creating spaces where medical information can be accurately conveyed and heard, requires research from diverse perspectives

In recent years, noise in Neonatal Intensive Care Units (NICUs) has become a source of stress for newborns, raising concerns and prompting calls for its reduction [1].

Shimura et al. examined the intrauterine sound environment—which can be considered the most comfortable and fundamental auditory setting for humans—as well as how sound is transmitted into the womb [2]. Yamaguchi et al. focused on intrauterine-transmitted sounds from the external environment as a component of the incubator's acoustic environment. They studied the effects of such sounds on infant behavioral development and developed a voice transformation system that presents sounds modified to resemble intrauterine sounds to infants inside incubators[3].

However, while there have been investigations from medical perspectives, few concrete attempts have been made from an engineering standpoint to reduce noise. Although noise intrusion from outside the incubator poses a problem, the acoustic characteristics of the incubator interior—such as resonance frequencies and internal sound pressure levels—have yet to be thoroughly understood. Moreover, effective methods for sound suppression have not been adequately explored.

Previous studies have been conducted by Koyama et al. on the acoustic characteristics of room spaces in healthcare facilities[4]. Additionally, research by Koizumi et al. has focused on the sound absorption properties in non-rectangular reverberation chambers [5]. The conventional JIS standard (A 1409) for measuring sound absorption coefficients requires large-scale acoustic equipment, such as reverberation chambers with volumes of 200m³ or more and sample areas of 12m² or larger, which incurs significant costs [6]. Furthermore, there are various measurement methods for sound absorption coefficients, such as using acoustic tubes or reverberation chambers, and the results vary depending on the method [7].

Therefore, when attempting to reduce the sound pressure level inside incubators using sound-absorbing materials, the issue arises as to which sound absorption coefficient data should be used. As far as the authors are aware, no research has been conducted on the acoustic characteristics of sound fields in such tightly enclosed small spaces.

This study aims to determine the resonance frequency of small, enclosed spaces (hereinafter referred to as "room spaces"), the acoustic damping ratio that controls the sound pressure level at the resonance frequency, and the sound absorption coefficient that suppresses the sound pressure level inside the room space.

To measure the sound absorption coefficient, we attempted to calculate the reverberation time in a room with sound-absorbing material attached to its walls, and used Eyring's formula [8] to derive the coefficient.

As a result, the sound absorption coefficient obtained by the conventional method showed a tendency to increase with higher frequencies, while the results from our approach were less dependent on frequency. However, we found that the sound absorption coefficient of the material itself still depended on frequency, and that the values obtained from our method were smaller than those obtained by conventional methods.

II. Experimental Method

Figure 1 shows the acrylic case used in the experiment. The dimensions are 1070 mm × 400 mm × 400 mm. Figure 2 illustrates the procedure for measuring the sound pressure level inside the room space.

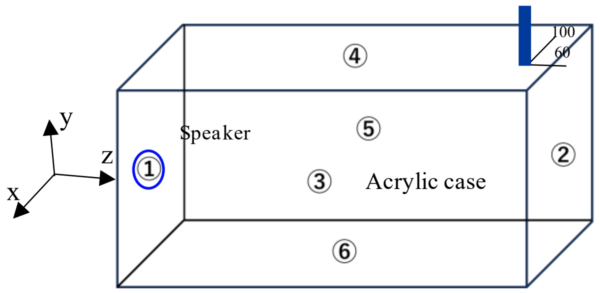

Fig. 1. Acrylic case used in this experiment.

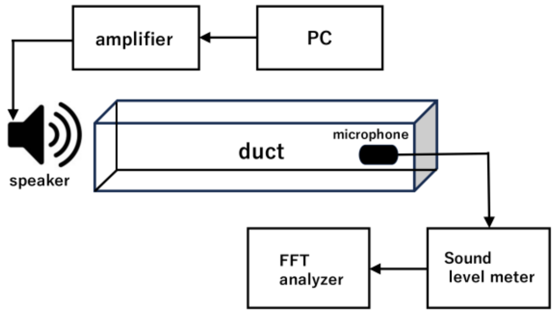

Fig. 2. Measurement diagram of SPL inside room.

These dimensions were set based on the standard size range (length, width, height) of incubators available on the market. However, since the actual dimensions of incubators vary by manufacturer, these dimensions were used as an example of a small enclosed space similar to an incubator. The measurements were performed according to the following steps.

(1). White noise was generated from a PC and delivered to the room space through a speaker via an amplifier (the sound level was kept constant).

(2). A room space of 400 mm (height) × 400 mm (width) × 1070 mm (depth) was constructed using 5 mm thick acrylic panels. The speaker was connected to the center of the 400 mm × 400 mm surface, and white noise was emitted. The sound pressure level was measured by a microphone placed at a 60 mm × 100 mm position at the edge of the opposite surface, and FFT analysis was performed. The FFT analysis was conducted for frequencies ranging from 2.5 Hz to 20,000 Hz at 2.5 Hz intervals, with a sampling frequency of 48 kHz. (3). Measurements were conducted for two conditions: one with no sound-absorbing material in the room space and another with sound-absorbing material (5t and 10t thickness) attached to the surfaces ①, ②, ③, ④, and ⑤ of the room space. In each case, three measurements were taken to verify reproducibility. The sound-absorbing material used was Calmflex F-2 (Inoac Corporation). (4)From the measurement results, the acoustic damping ratio was calculated using the half-value width method. The measurement patterns are as follows, where the numbers in parentheses indicate the area of the sound-absorbing material:

a) No sound-absorbing material attached
b) Surface ① (0.16 m²)
c) Surfaces ① and ② (0.32 m²)
d) Surfaces ①, ②, and ③ (0.72 m²)
e) Surfaces ①, ③, ④, and ⑤ (1.36 m²)

The reverberation time measurements were conducted as follows:

Figure 3 shows the method for measuring reverberation time.

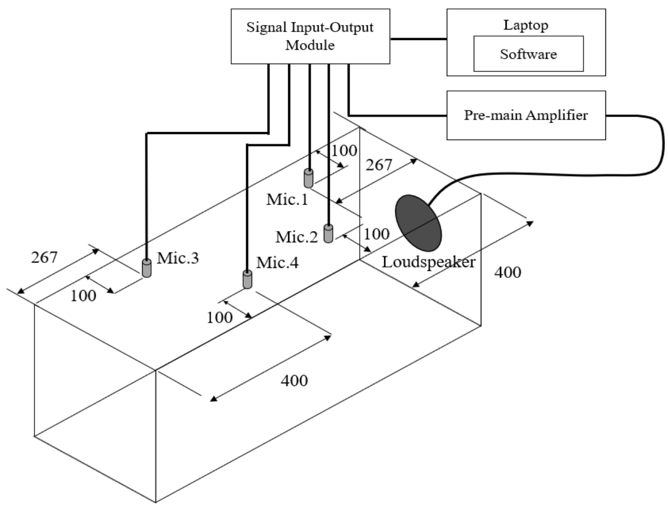

Fig. 3. Measurement diagram of reverberation time.

As illustrated in Figure 3, pink noise was output from a speaker (Fostex FF85WK) via a pre-main amplifier (Denon PMA-600NE) controlled by software (Amp & B&K PULSE Reverberation Time) on a PC. The sound from the speaker was recorded by a microphone (B&K 4190 model) and a signal input-output module (Amp & B&K 3160-A-042 model) after the pink noise was stopped.

The recorded reverberant sound was analyzed using the aforementioned software, and the reverberation time for each octave band frequency (the time it takes for the sound pressure level to decay by 60 dB from the steady state) was calculated. The time to decay by 60 dB from the steady state was derived using a linear regression formula based on the least squares method. In this study, the average reverberation time calculated from measurements taken by four microphones was used for evaluation.

When setting up the microphones, openings capable of fitting a 1/4-inch microphone were created, and the 1/4-inch microphones were installed into these openings. To prevent sound leakage from the gap, the space between the microphone and the opening was sealed with clay. The microphones were placed at a certain distance from the wall, positioned randomly, and arranged to ensure accurate measurements.

III. Experimental Results and Consideration

A. Reproducibility of Experimental Result

As an example of the experimental case, the frequency characteristics of the sound pressure level inside the room space with no sound-absorbing material are shown in Figure 4. This figure overlays the results from three trials conducted under the same conditions. Since the results overlap almost completely, reproducibility was confirmed. The same was true for the other cases as well.

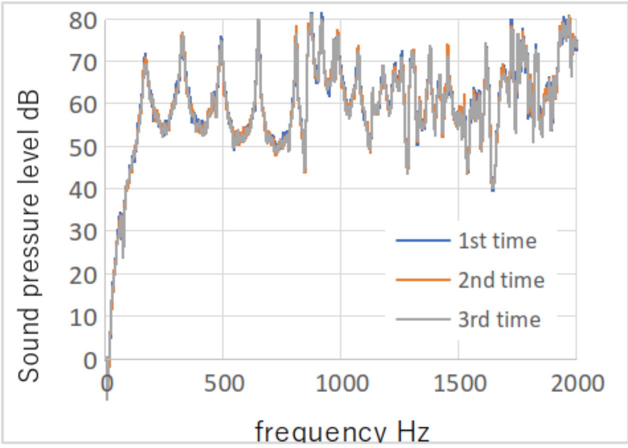

Fig. 4. Frequency spectrum showing reproducibility.

B. Experimental Result in case of without Absorbent

(1) Resonant Frequency

The resonance frequency was determined by reading the frequency of the peak sound pressure level from the FFT analysis results obtained from measurements without sound-absorbing material. To obtain a more accurate resonance frequency, the frequency was varied in 1 Hz increments using a signal generation software to confirm the peak of the acoustic level, thus obtaining a more precise resonance frequency. The results are shown in Table 1. Table 1 presents the three measurement results for each mode, the average values, and the high-precision (shaded) resonance frequencies.

From Table 1, it can be seen that there is almost no error in the three measurements, confirming the reproducibility of the results.

(2) Resonant Mode

Next, pure tones corresponding to each resonance frequency shown in Table 1 were applied, and the sound pressure levels were measured to investigate the resonance modes by determining the maximum and minimum sound pressure levels. These results are presented in Table 2. The mode measurements were conducted in an acrylic case, where, at each resonance frequency, a microphone was swept across the x-axis, y-axis, and z-axis of the case, measuring the sound pressure variations between the edges.

TABLE 1. Resonant frequency without sound absorbing material.

Mode No.	1st time	2nd time	3rd time	average	High precision value
1	182	177	180	179	174
2	332	332	335	333	324
3	490	495	487	490	493
4	652	652	652	652	650
5	810	807	807	808	812

The resonance frequencies for each mode in the three-dimensional space are given by the following calculation formula [8].

$$f_{l,m,n} = \frac{c}{2}\sqrt{\left(\frac{l}{l_x}\right)^2 + \left(\frac{m}{l_y}\right)^2 + \left(\frac{n}{l_z}\right)^2} \quad (1)$$

Where,

f: Resonance frequency [Hz], c: Speed of sound in air [m/s], l: Mode number in the x-axis direction of the room space, l_x: Length of the room space in the x-axis direction [m], m: Mode number in the y-axis direction of the room space, l_y: Length of the room space in the y-axis direction [m], n: Mode number in the z-axis direction of the room space, l_z: Length of the room space in the z-axis direction [m], l, m, n: Integers. The speed of sound is assumed to be 346 m/s (at room temperature of 25℃).

Table2 shows the comparison between calculation and experimental results of the resonant frequencies.

From this, it can be seen that the calculated values closely match the measured results.

TABLE 2. Comparison between Cal. and Exp. of Resonant Frequency.

Mode No.	Mode (l,m,n)	Cal.	Exp.
1	(0,0,1)	162	174
2	(0,0,2)	324	324
3	(0,0,3)	487	493
4	(0,0,4)	649	650
5	(0,0,5)	810	812

The reason that only the mode in the duct length direction appeared is that, due to the position and orientation of the speaker, only that mode was excited.

C. Experimental Result in case of with Absorbent

(1) Effect of Absorbent to Sound Pressure Level

The FFT analysis was conducted three times each for the room space with sound-absorbing materials of thickness 5t and 10t, as described in section 2, with frequency analysis up to 5000 Hz at 2.5 Hz intervals. The results are shown in Figures 5(a) and 5(b), respectively.

The legend in the figure indicates the area of the sound-absorbing material applied.

Clear peaks are observed up to the 5th mode (below 1000 Hz), but higher modes have closely spaced resonance frequencies, making it difficult for them to appear clearly. In this space, modes are prominent in frequency bands below 1000 Hz, while modes do not appear above this frequency range

From the graphs in Figure 5, the resonance frequencies are 175 Hz, 325 Hz, 490 Hz, 645 Hz, and 810 Hz. These values closely match the previously calculated resonance frequencies. It appears that the frequency range where modes appear corresponds to the frequency range where plane waves are formed ($f = c / l_x = 346 / 0.4 = 865$ Hz). Furthermore, it was

Kunihiko Ishihara, Yuka Yamashita, and Yuki Oe, "On Absorbing Coefficient and Acoustic Damping Ratio of Closed Small Space," *International Research Journal of Advanced Engineering and Science*, Volume 11, Issue 1, pp. 8-16, 2025.

confirmed that the thicker the sound-absorbing material and the larger the applied area, the lower the sound pressure level. Therefore, for the cases where resonance frequencies were identified (5t and 10t), the sound pressure levels at each resonance frequency (peak sound pressure level) are shown in Figure 6.

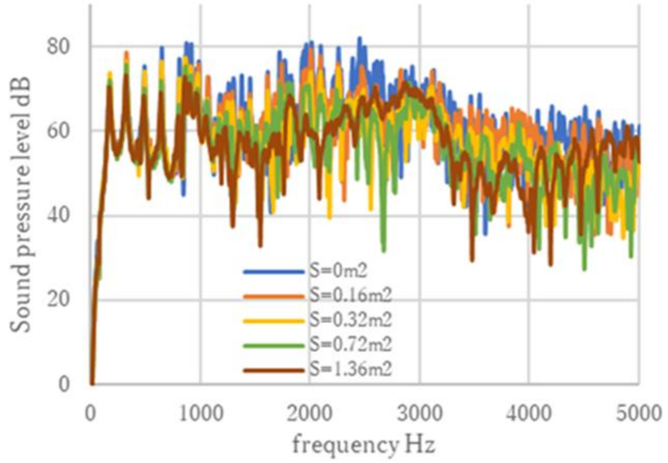

(a) 5t

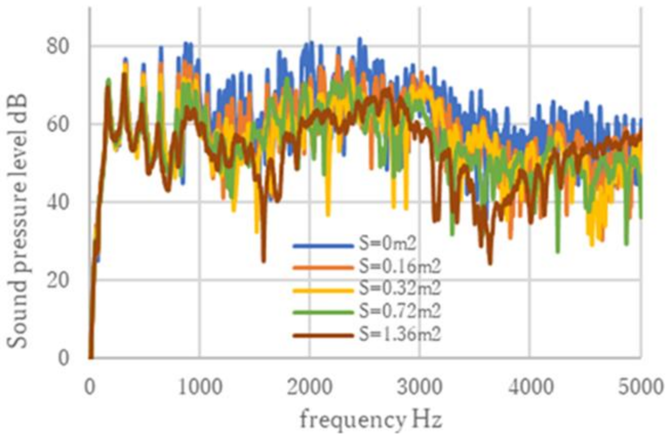

(b) 10t

Fig. 5. Sound pressure level in case of various amount of sound absorbing material.

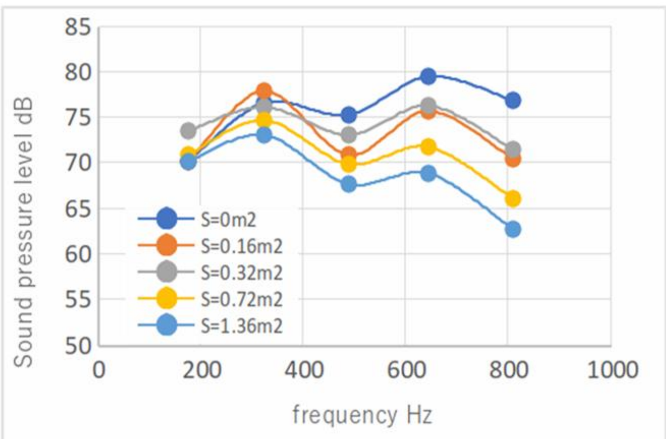

(a) 5t

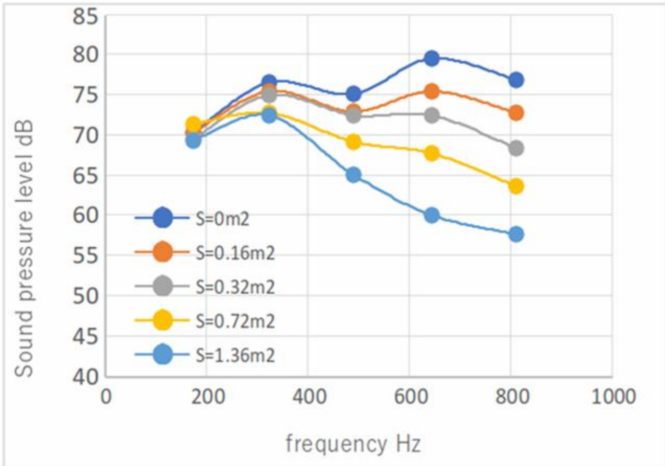

(b) 10t

Fig. 6. Sound pressure level at resonant frequencies in case of sound absorbing material.

The parameter is the area of the applied sound-absorbing material. As the amount of sound-absorbing material increases, or in other words, as the absorption power A=Sα (where S is the absorption area and α is the average absorption coefficient) becomes larger, the peak sound pressure level tends to decrease.

Additionally, it can be observed that higher modes are more influenced by the absorption power.

Figures 7(a) and (b) show the relationship between the area of the applied sound-absorbing material and the overall sound pressure level (O.A. SPL) for sound-absorbing material thicknesses of 5t and 10t, both theoretically and experimentally

Theoretical values were calculated assuming that the SPL at S=0.95 m^2 matches the experimental values, and that when the area doubles, the SPL decreases by 3 dB. In both thickness cases, the theoretical and experimental values align well. Therefore, these results can be considered valid.

(2) Effect of Thickness of Absorbent to Resonant Frequency

Although not shown here, a comparison was made of the resonance frequencies when a 20mm thick sound-absorbing material was applied to surfaces ① and ② in Figure 1.

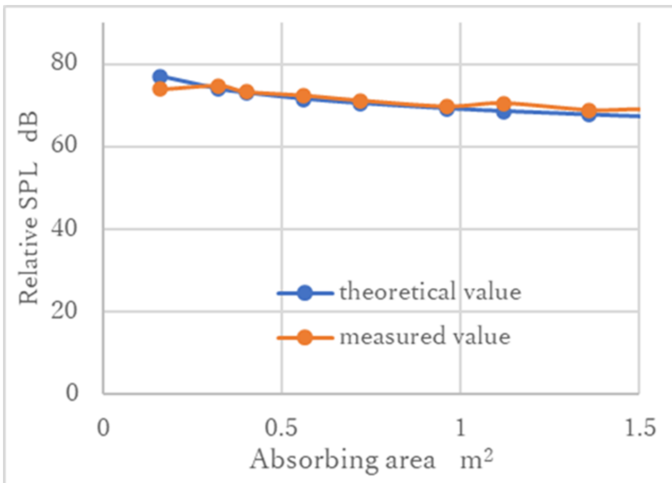

(a) 5t

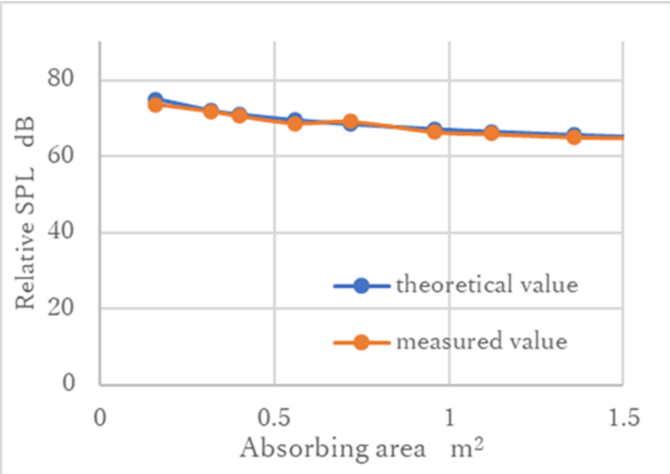

(b) 10t

Fig. 7. Sound pressure level at resonant frequencies in case of sound absorbing material.

It is hypothesized that the resonance frequency would increase due to the reduction in space dimensions caused by the installation of the sound-absorbing material.

The peaks shown in Figure 5 correspond to the modes in the longitudinal direction, so if a 20mm thick sound-absorbing material is applied to the longitudinal dimension of 1070mm, the length would be reduced to 1030mm.

In this case, using the formula f=c/2L, the ratio 1070/1030=1.039, meaning the resonance frequency is expected to increase by 3.9%.

Specifically, the frequencies are expected to shift as follows:
The 1st mode: 174 Hz → 181 Hz
The 2nd mode: 324 Hz → 337 Hz
The 3rd mode: 493 Hz → 512 Hz
The 4th mode: 650 Hz → 675Hz
The 5th mode: 812 Hz → 844Hz

The measured results, however, show that even with a 20mm thick sound-absorbing material, the outcome is almost identical to the case without any sound-absorbing material. Therefore, it can be said that the presence of sound-absorbing material has no significant effect on the resonant frequency.

D. Acoustic Damping Ratio

The acoustic damping ratio ζ was determined using the half-width method from Figure 5 shown in section C.

The acoustic damping ratio can be expressed by the following formula (2) when f_0 is the peak frequency and f_1 and f_2(where $f_2>f_1$) are the frequencies at which the sound pressure level drops 3 dB below the peak frequency.

$$\zeta = \frac{f_2 - f_1}{2f_0} \tag{2}$$

Using formula (2), the acoustic damping ratios were calculated for the sound-absorbing materials with thicknesses of 5t and 10t up to the 5th mode, and the results are shown in Figures 8(a) and (b).

From these results, it was clearly observed that as the absorption area increases, the acoustic damping ratio increases, and as the mode order increases, the acoustic damping ratio decreases.

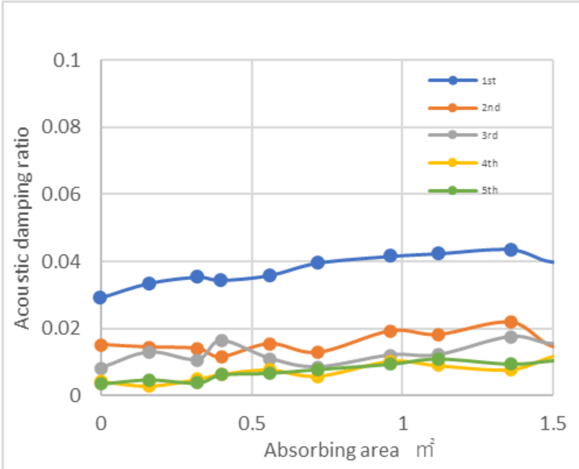

(a) 5t

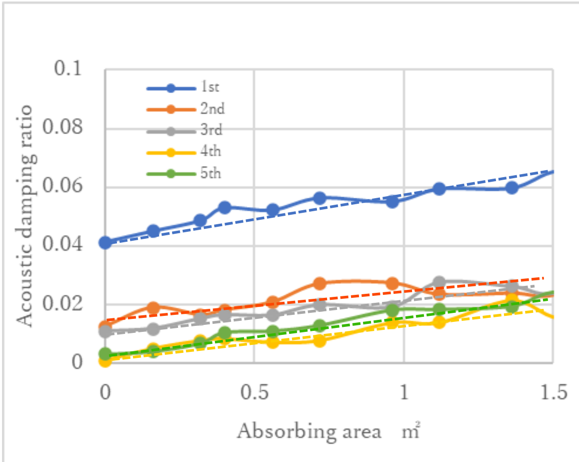

(b) 10t

Fig. 8. Acoustic damping ratio in case of sound absorbing material of 5t and 10t.

For Figure 8(b), the acoustic damping ratios ζ for the mode orders at applied areas of 0.5 m², 1.0 m², and 1.5 m² were calculated, and the product of each mode's natural acoustic frequency f_n and ζ was determined. The coefficient of variation was then calculated from the mean and standard deviation of the $f_n \cdot \zeta$ values for each mode, as shown in Table 3.

TABLE 3. Coefficient of variation for data of fn ・ ζ.

Mode order	fn	ζ at 0.5m²	ζ at 1.0m²	ζ at 1.5m²	fn・ζ at 0.5m²	fn・ζ at 1.0m²	fn・ζ at 1.5m²
1	174	0.048	0.056	0.062	8.35	9.74	10.7
2	324	0.02	0.027	0.030	6.48	8.75	9.72
3	493	0.016	0.021	0.026	7.89	10.3	12.8
4	650	0.008	0.014	0.021	5.20	9.10	13.6
5	812	0.009	0.015	0.020	7.31	12.1	16.2
	Mean of fn・ζ				7.05	10.0	12.6
	Standard deviation of fn・ζ				1.11	1.21	2.27
	Coefficient of variation				0.158	0.121	0.180

Since the coefficient of variation is between 0.12 and 0.18, the product of the natural acoustic frequency and the acoustic damping ratio for each mode can be considered approximately constant. This result matches the reference[10].

In the theory of viscous damping vibrations, $c/m=2\zeta\omega_n$, , so this result is considered valid.

Here, c and m are the viscosity damping coefficient and mass, respectively, both constant, ζ is the viscosity damping ratio, and ω_n is the natural angular frequency.

Here, the mean value is $\bar{x} = \frac{1}{N}\sum_{i=1}^{N} x_i$,

the standard deviation is $S.D. = \sqrt{\frac{1}{N}\sum_{i=1}^{N}(x_i - x)^2}$

and the coefficient of variation is $C.V. = S.D./\bar{x}$

E. Measurement of Indoor Sound Absorption Coefficient due to Reverberation Time

This section attempts to determine the absorption coefficient of the acoustic material applied to a confined small space. To calculate the absorption coefficient using Eyring's formula, FFT analysis was conducted with frequency analysis performed in 2.5 Hz intervals up to 5000 Hz. The reverberation time was determined using the method described in Chapter II, and the absorption coefficient was calculated using the Eyring formula shown below.

$$T = \frac{0.161V}{-S\log_e(1-\bar{\alpha})} \quad (3)$$

Where,

T: Reverberation time (s), *V*: Room volume (m³), α: Average absorption coefficient, *S*: Total surface area of the room (m²). Figures 9(a) and (b) show the absorption power when acoustic materials with thicknesses of 5t and 10t are applied. The legend indicates the absorption area. As the applied absorption area increases, the absorption power *A* increases. This is consistent with *A*=*S*α. However, the frequency characteristics differ from the results of the conventional reverberation chamber method.

Therefore, although not for small spaces, experimental results of the reverberation time in a nursery room (volume:95 m³, surface area: 130 m², absorption material area: 20 m²) with absorption material (glass wool board: thickness 25 mm, density 80 kg/m³, glass fiber covering) applied to the ceiling were measured. These results are shown in Figure 9. In the figure, "4age" refers to a 4-year-old child, and "before" and "after" indicate measurements before and after the application of the absorption material.

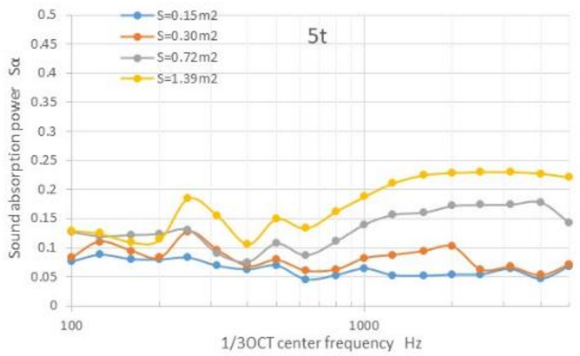

(a) 5t

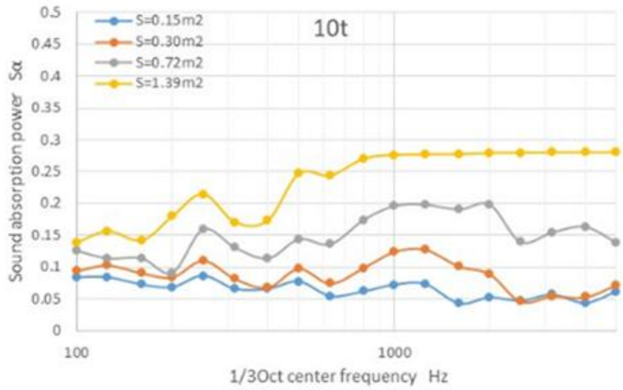

(b) 10t

Fig. 9. Sound absorption power in cases of 5t and10t thickness.

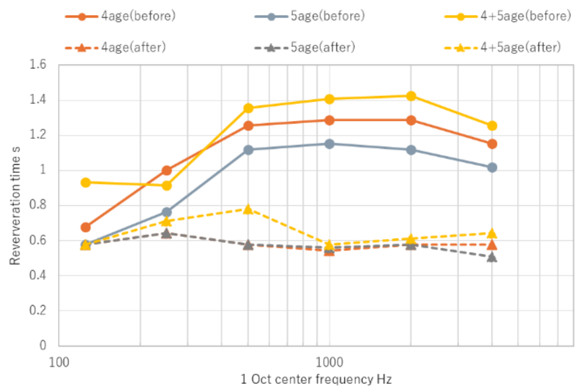

Fig. 10. Reverberation time of nursery room provided by Miwa[9].

From these results, it can be observed that the frequency characteristics of the reverberation time remain almost constant above 500 Hz. When absorption coefficients are calculated using the Eyring's formula or Sabine's formula, it is inferred that the absorption coefficient does not depend on frequency. In this study, the absorption coefficient was calculated using Eyring's formula. First, the reverberation time was measured, and then the absorption coefficient was determined using Equation (3).

Since the absorption coefficient of the absorption material is the same when the material and thickness are identical, the average absorption coefficient was calculated by averaging the absorption coefficients for four different absorption areas described in Chapter II. The results are shown in Figure 11. From this figure, it can be seen that as the thickness of the absorption material increases, the absorption coefficient increases. Furthermore, the absorption coefficient, as expected, shows little dependence on frequency. In general, the absorption characteristics of the material depend on frequency, with the absorption coefficient increasing as the frequency rises. Figure 12 compares the absorption coefficient from this experiment with the manufacturer's (Inoac Corporation) catalog values. In this comparison, the 10t material is considered. The new experimental results suggest that, in small spaces like the one in this study, the absorption coefficient does not depend on frequency. However, it should be noted that this result is not the absorption coefficient of the material itself.

International Research Journal of Advanced Engineering and Science
ISSN (Online): 2455-9024

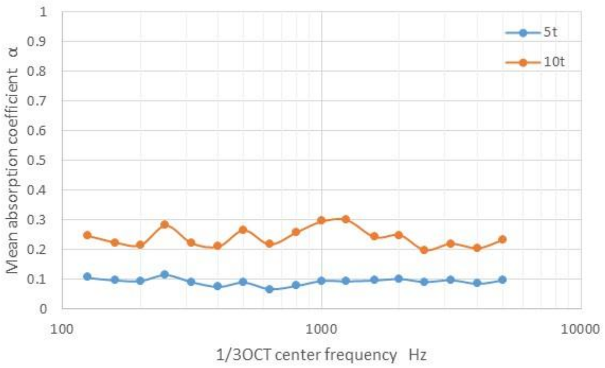

Fig. 11 Absorption coefficient of material.

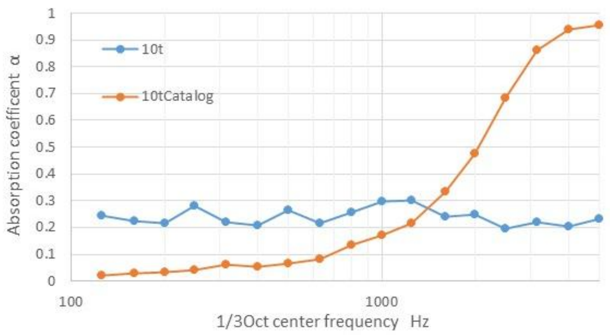

Fig. 12. Comparison of absorption coefficient between catalogue value and present result.

IV. Comparison of Room Sound Pressure Levels Using Catalog and Measured Absorption Coefficients and Their Measured Values

To further confirm the validity of the absorption coefficient obtained in the previous section, we conducted an analysis using the case of an absorption material thickness of 10t. The absorption coefficients from the catalog and measured values on indoor acoustical theory. These results were then compared with the steady-state sound pressure level of the room when determining the reverberation time. In this case, the frequency characteristics of the sound pressure level in the room without any absorption material were used as the sound source. The results are shown in Figure 13.

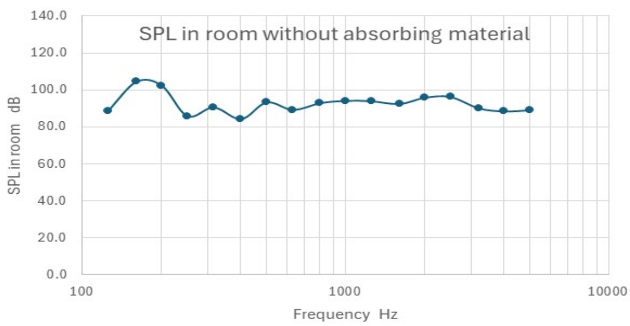

Fig. 13. Power level of noise source assumed.

This is the power average value of the sound pressure level measured with four microphones in a room without acoustic treatment when calculating the reverberation time. The values in Figure 13 were used as the acoustic power level LW and the sound pressure level of the room with acoustic treatment was calculated using the indoor acoustical theory formula (4):

$$L_p = L_w + 6 - 10\log R \qquad (4)$$

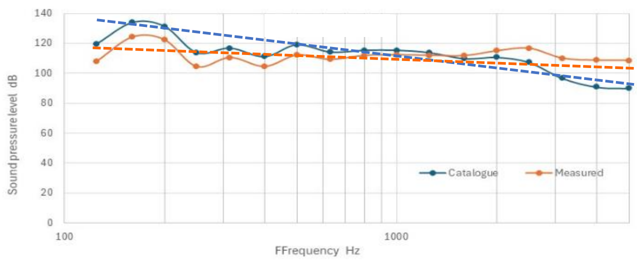

(a) 5t, S=0.15m^2

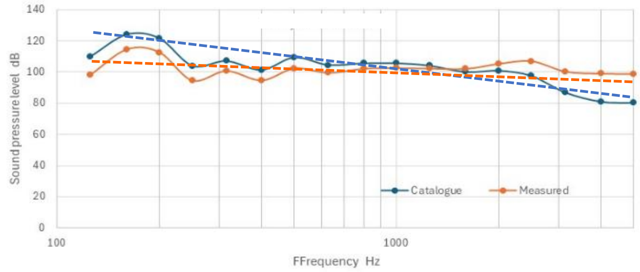

(b) 10t, S=1.39m^2

Fig. 14. Calculation result of SPL inside room.

where R is the room constant, given by $R=S\alpha/(1-\alpha)$. S and α represent the surface area of the applied absorption material and the average absorption coefficient, respectively.

The calculation results for the absorption material application areas of 0.15 m² and 1.39 m² are shown in Figures 14(a) and(b), respectively.

The blue lines represent the calculation results using the catalog values for the absorption coefficient, while the orange lines represent the results calculated using the measured absorption coefficients obtained from the reverberation time measurements. The dashed lines indicate the approximate straight lines. Both the frequency characteristics of the absorption coefficients are the same, with only the applied absorption area differing. Therefore, they show the same frequency characteristics, with the levels differing by 10log(1.39/0.15) = 9.7 dB, as expected. Additionally, when looking at the absorption coefficient at 10t in Figure 12, it intersects around 1300 Hz. As a result, the calculated indoor sound pressure levels also intersect with the catalog values and the measured values at the same frequency, which is reasonable. Moreover, the inversion of sound pressure levels before and after the intersection frequency coincides with the inversion of the absorption coefficients. The measured indoor sound pressure levels are shown in Figures 15(a) and (b), respectively. The difference between the calculated values and the measured sound pressure levels arises because the power level of the sound source was replaced with the indoor sound pressure level in the case without absorption material.

Therefore, the absolute values of the sound pressure levels are not discussed here, and only the frequency characteristics are compared between the calculated and measured values.

Kunihiko Ishihara, Yuka Yamashita, and Yuki Oe, "On Absorbing Coefficient and Acoustic Damping Ratio of Closed Small Space," *International Research Journal of Advanced Engineering and Science*, Volume 11, Issue 1, pp. 8-16, 2025.

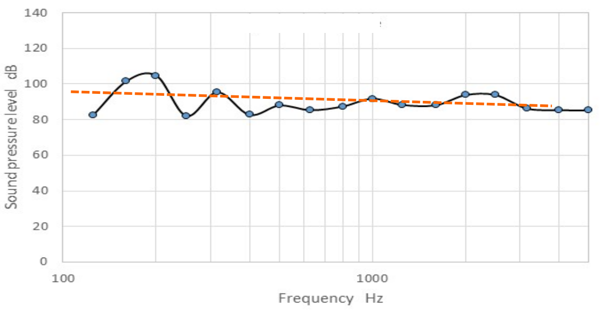

(a) 10t, S=0.15m^2, Ave.

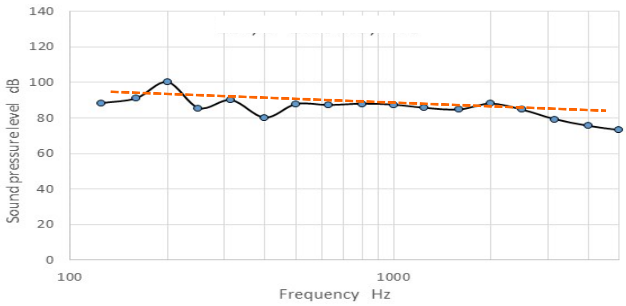

(b) 10t, S=1.39m^2, Ave

Fig. 15. Calculation result of SPL inside room.

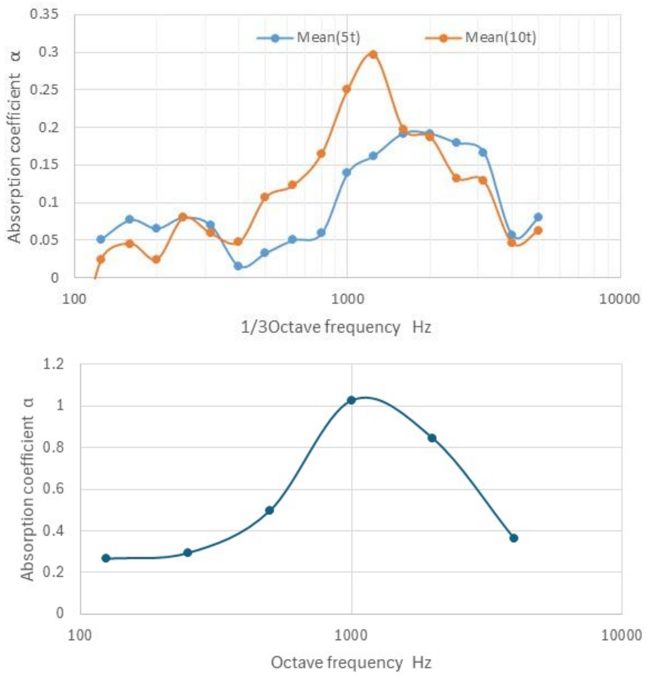

Fig. 16. Absorption coefficient of acoustic absorbent itself.

Since the frequency characteristics of the indoor sound pressure levels using the measured absorption coefficients match well with the measured sound pressure levels, it can be concluded that the measured absorption coefficients are reasonable.

V. On Absorption Coefficient of Absorbent Itself

Until now, we have discussed the absorption coefficient of the treated indoor space. To determine the absorption coefficient of the absorption material used, we calculate the absorption power before and after the treatment, using the reverberation time and Sabine's equation, and then divide the difference by the absorption area *S*. In other words, the absorption coefficient of the material used can be determined using Equation (5):

$$\alpha = \left(A_{after} - A_{before}\right)/S \tag{5}$$

The absorption coefficient of the material obtained in this way is shown in Figure 16(a). For reference, the absorption coefficient of the material obtained from the data of Miss. Miwa in Figure 10 is shown in Figure 16(b). The frequency characteristics of both are quite similar, and Figure 16(a) shows that as the thickness of the material increases, it shifts towards the lower frequencies, representing the typical absorption material characteristic.

From the above analysis, it can be concluded that the absorption coefficient of the indoor space shows little frequency dependence, while the absorption coefficient of the material itself has a peak around 1000 Hz. Furthermore, the absorption coefficient of the material measured in small spaces tends to be lower than that obtained by conventional methods.

VI. Conclusion

Experiments and analyses were conducted to clarify the noise reduction effects of sound-absorbing materials in closed small spaces such as incubators. The following findings were obtained:

(1) In the low and middle frequency ranges (100–1000 Hz), acoustic modes of the sound field are generated within the space, while in the high-frequency range, the field becomes diffusive. As sound suppression factors, in the former case, the acoustic damping ratio is important, while in the latter case, the absorption coefficient plays a key role. The frequency range where peaks occur corresponds to the frequency range where plane waves are valid.

(2) Regarding the characteristics of the acoustic damping ratio, it decreases as the mode order increases, and the relationship between the damping ratio and mode frequency is that the product of the both is constant.

(3) The absorption coefficient of the closed small space was attempted to be determined using the reverberation time and the Eyring formula. The results showed that the absorption coefficient is independent of frequency. This is also demonstrated in the literature (Miwa), and it can be inferred that the absorption coefficient obtained from this result matches the measured internal sound pressure level in the nursery room calculations. However, the absorption coefficient of the sound-absorbing material itself exhibits a peak around 1000 Hz. Also, the absorption coefficient of the material measured in small spaces tends to be lower than the absorption coefficient obtained using conventional methods.

(4) The thickness of the sound-absorbing material does not affect the resonance frequency. In other words, for a duct of length L (m) with sound-absorbing material of thickness t

(m) applied at both ends, the resonance frequency is given by c/2L, not c/2(L−2t).

REFERENCES

[1] Y. Oto, "Improvement Example of Sound Insulation Effect of Incubator Cover in NICU", Master's thesis, Mie University, 2020. (in Japanese).

[2] Y. Shimura, I. Yamauchi and H. Fukuhara, "Sound Environment Surrounding the Fetus", INCE-Japan, Vol.15, No.4. (1989), pp.197-201. (in Japanese).

[3] Y. Yamaguchi, N. Odagiri, K. Ikeda, Y. Shimura, T. Hashimoto and M. Wada, "The Effect of Sounds on Neonates in an infant Incubator", Japanese Society of Medical Instrumentation NII-Electronic Library Service J, Vol.69, No.8 (1989), pp.378-383. (in Japanese).

[4] Y. Koyama, "Investigation on a sound environment for making more effective and functional use of each room in medical acilities", Grants-in Aid for Scientific Research, Research Result Report, Assignment Number:15K15255. (in Japanese).

[5] H. Koizumi, A. Matsuoka, M. Kobayashi and Y. Kawai, "A Basic Study on a Sound Absorber using the Tubular Cavity Resonance", Toda Corporation, Technical Research Institute, No.40, 2014, pp.1-4. (in Japanese).

[6] H. Yoshida, H. Suzuki and A. Omoto, "A study on absorption coefficient mesurement in small reverberation chamber, Acoustical Society of Japan, Kyusyu branch, http://asj-kyushu.acoustics.jp.(in Japanese).

[7] S., Sugie, "A variety of measuring methods for sound absorption coefficient ; Difference among measured results of at normal, oblique and random incidences", The Journal of the Acoustical Society of Japan, Vol.66, No.6, 2020, pp.270-275. (in Japanese).

[8] K. Shiraki, "Design of noise protection and simulation", Oyogijyutsu syuppan, p.33, 1987(in Japanese).

[9] H. Miwa, "Research on Improvement Efect of Sound Environment of Nuesery Room due to Ceiling Sound Absorption", Summary Collection of Graduation thesis 2018, Department Architecture, University of Tokyo.

[10] K. Ishihara, A. Goto and M. Kashino, "Relation between peak value and acoustic damping of sound pressure level of one dimensional sound field partitioned with perforated plates", International Journal of Engineering and Applied Sciences, Vol.6, Issue.9,pp.1-5, 2019